Exisulind-induced Apoptosis in a Non-Small Cell Lung Cancer Orthotopic Lung Tumor Model Augments Docetaxel Treatment and Contributes to Increased Survival

Clark M. Whitehead,[1] Keith A. Earle, John Fetter, Songmei Xu, Theresa Hartman, Daniel C. Chan, Tom L. M. Zhao, Gary Piazza, Andres J. P. Klein-Szanto, Rifat Pamukcu, Hector Alila, Paul A. Bunn, Jr., and W. Joseph Thompson

Cell Pathways, Inc., Horsham, Pennsylvania 19044 [C. M. W., K. A. E., J. F., S. X., T. H., G. P., R. P., H. A., W. J. T.]; University of Colorado Health Sciences Center, Division of Medical Oncology, Denver, Colorado 80262 [D. C. C., T. L. M. Z., P. A. B.]; and Fox Chase Cancer Center, Philadelphia, Pennsylvania 19111 [A. J. P. K-S.]

Abstract

We reported previously a significant increase in survival of nude rats harboring orthotopic A549 human non-small cell lung cancer tumors after treatment with a combination of exisulind (Sulindac Sulfone) and docetaxel (D. C. Chan, Clin. Cancer Res., *8*: 904–912, 2002). The purpose of the current study was to determine the biochemical mechanisms responsible for the increased survival by an analysis of the effects of both drugs on A549 orthotopic lung tumors and A549 cells in culture. Orthotopic A549 rat lung tissue sections from drug-treated rats and A549 cell culture responses to exisulind and docetaxel were compared using multiple apoptosis and proliferation analyses [*i.e.,* terminal deoxynucleotidyl transferase-mediated nick end labeling, active caspase 3, the caspase cleavage products cytokeratin 18 and p85 poly(ADP-ribose) polymerase, and Ki-67]. Immunohistochemistry was used to determine cyclic GMP (cGMP) phosphodiesterase (PDE) expression in tumors. The cGMP PDE composition of cultured A549 cells was resolved by DEAE-Trisacryl M chromatography and the pharmacological sensitivity to exisulind, and additional known PDE inhibitors were determined by enzyme activity assays. Exisulind inhibited A549 cell cGMP hydrolysis and induced apoptosis of A549 cells grown in culture. PDE5 and 1 cGMP PDE gene family isoforms identified in cultured cells were highly expressed in orthotopic tumors. The *in vivo* apoptosis rates within the orthotopic tumors increased 7–8-fold in animals treated with the combination of exisulind and docetaxel. Exisulind increased the *in vivo* apoptosis rates as a single agent. Docetaxel, but not exisulind, decreased proliferative rates within the tumors. The data indicate that exisulind-induced apoptosis contributed significantly to the increased survival in rats treated with exisulind/docetaxel. The mechanism of exisulind-induced apoptosis involves inhibition of cGMP PDEs, and these results are consistent with a cGMP-regulated apoptosis pathway.

Introduction

Exisulind (Sulindac Sulfone, Aptosyn) is an antineoplastic drug being developed for the treatment of premalignant and malignant cancer. It is the lead drug of a family of compounds termed selective apoptotic antineoplastic drugs because they induce apoptosis in neoplastic but not normal cells. Exisulind has been shown to selectively induce apoptosis in cell lines derived from many cancers including colon, bladder, prostate, and breast (1–4). The drug also inhibits tumor growth in rodent models of mammary, bladder, prostate, and colon carcinogenesis (1, 3, 5, 6). In colon cancer cells exisulind induces apoptosis by a mechanism that involves the inhibition of cGMP[2] phosphodiesterases, including PDE 2 and 5, activation of PKG and phosphorylation of selective substrates (7). Many cancers, including colon, pancreatic, lung, and bladder, have high levels of cGMP PDE compared with normal tissue (3, 8–10). Exisulind treatment of colon tumor cells in culture results in a sustained increase in intracellular cGMP levels that results in the activation of PKG (11, 12). Activated PKG directly phosphorylates mitogen-activated protein kinase kinase kinase 1, which leads to the activation of Jun kinase 1 and the initiation of apoptosis (13, 14). In addition, PKG phosphorylates β-catenin causing a reduction in its accumulation and anti-apoptotic effects (15).

Lung cancer is currently the leading cause of cancer death in the United States (16). Even with recent advances in treatment, response and remission rates remain unacceptably low. Whereas docetaxel treatment of NSCLC produces a modest improvement in survival (17–20), there remains a need for novel agents to improve the treatment and survival of NSCLC patients. A previous *in vitro* study reported that the combination of exisulind and paclitaxel produced a synergistic inhibition of growth in a variety of lung cancer cell lines (21). We reported recently the results of a study investigating the efficacy of exisulind and docetaxel treatment, alone or in

Received 10/22/02; revised 2/10/03; accepted 2/19/03.

[1] To whom requests for reprints should be addressed, at Cell Pathways, Inc., 702 Electronic Drive, Horsham, PA 19044. Phone: (215) 706-3800; Fax: (215) 706-3801; E-mail: cwhitehead@cellpathways.com.

[2] The abbreviations used are: cGMP, cyclic G; PDE, phosphodiesterase; PKG, protein kinase G; NSCLC, non-small cell lung cancer; PARP, poly-(ADP-ribose) polymerase; IHC, immunohistochemistry; TUNEL, terminal deoxynucleotidyl transferase-mediated nick end labeling; GST, glutathione *S*-transferase; cAMP, cyclic AMP.

combination, in nude rats harboring orthotopic human A549 NSCLC tumors (22). We found that rats treated with the combination of exisulind (50 mg/kg/day) and docetaxel (5 mg/kg 6× or 5 mg/kg 3× reduced to 2.5 mg/kg 3×) had a 60% survival rate at the end of a 80-day study period. Conversely, untreated control rats or rats treated with each agent alone or in combination at a lower dose died at earlier time points (40–79 days). Lungs harvested from the above combination treatment groups at death or on sacrifice at the completion of the study displayed histological differences. Lungs harvested from rats treated with high dose combinations of exisulind/docetaxel had a reduction in both tumor mass and distal metastases compared with rats treated with either lower combination doses or each drug alone.

In our current study, these lung tissue specimens were additionally analyzed to determine the molecular mechanisms associated with the increase in survival observed previously. Tissue samples were labeled to determine the level of cGMP PDEs 5 and 1, apoptosis levels and proliferative rates within the *in vivo* orthotopic tumors. These data were supplemented by *in vitro* experiments on cultured human A549 NSCLC cells that determined cGMP PDE enzymatic activity and apoptosis levels. Comparing the effects of exisulind on A549 cells both in culture and within *in vivo* orthotopic tumors resulted in an additional understanding of its biological effects alone or in combination with docetaxel.

Materials and Methods

Cell Culture. The NSCLC line, A549, was obtained from the American Type Culture Collection (Rockville, MD) and maintained in F12K medium (Invitrogen, Carlsbad, CA) supplemented with 5% FCS, 1% glutamine, and 1% antibiotic/antimycotic solution. Cell cultures were grown in 5% CO_2 with 100% humidity.

Exisulind and Docetaxel. Exisulind was provided by Cell Pathways, Inc. (Horsham, PA) and docetaxel by Aventis Pharmaceuticals (Bridgewater, NJ). Exisulind suspension was prepared for animal studies in 0.5% carboxymethylcellulose (low viscosity; Aldrich Chemical Company, Milwaukee, WI) and administered p.o. to the rats by single daily gastric gavage at doses of 25 or 50 mg/kg body weight. The stock solution of docetaxel was prepared in DMSO, and the working concentrations of 2.5 or 5.0 mg/kg were diluted in sterile water and injected i.p. once weekly for 5 or 6 consecutive weeks. For cell culture experiments, stock solutions of exisulind were prepared in 100% DMSO (500 mM) and diluted in growth medium with DMSO ≦0.1% or less.

Immunofluorescence. Subconfluent A549 cultures were treated, 24 h after seeding, with either DMSO alone (vehicle control) or exisulind as indicated. Floating cells were collected and pooled with adherent cells (detached by trypsin treatment). These total cell fractions were deposited on microscope slides with a Shandon cytospin (500 × *g* for 2 min). Cells to be labeled with antibodies to active caspase 3 and p85 PARP fragment (Promega, Madison, WI) were fixed in 3% paraformaldehyde for 10 min, and permeablized with 0.5% Triton-100 for 2 min and washed for 2 min in D-PBS. Cells to be labeled for caspase cleaved cytokeratin 18 using the M30 monoclonal antibody (Roche, Indianapolis, IN) were fixed for 30 min in −20°C methanol, air-dried, and rehydrated in D-PBS for 2 min. Primary antibodies were incubated as per the manufacturer's protocols. Cells were washed twice for 5 min each in D-PBS between each antibody incubation. A species-specific FITC or Cy3-conjugated secondary antibody was used to visualize the distribution of the primary antibody within the cells. Slides were counterstained with 4′,6-diamidino-2-phenylindole (0.5 μg/ml in D-PBS), mounted in Vectashield antifade solution (Vector Laboratories, Inc., Burlingame, CA) and observed using an Olympus IX-70 microscope. Digital images were collected using a Spot 2 camera (Diagnogstic Instruments, Sterling Heights, MI), annotated, and arranged in Adobe Photoshop 7.

PDE Isozyme Fractionation and Assay. A549 cells were cultured, as described above, to confluence in 20 150-cm^2 flasks. Approximately 400 million cells were manually homogenized in a buffer containing 20 mM Tris acetate, 5 mM magnesium acetate, 0.1 mM EDTA, 1.0% Triton X-100, and protease inhibitors (10 mM benzamidine, 10 μM tosyl-lysylchloromethylketone, 20 nM aprotinin, 2 μM leupeptin, and 2 μM pepstatin A) at pH 7.5 using a glass tissue grinder with a Teflon pestle. After ultracentrifugation at 100,000 × *g* at 4°C for 1 h, the supernatant was diluted 5-fold with a lower salt form of the homogenation buffer containing 5 mM Tris acetate and no Triton X-100. This sample was loaded at 1 ml/min onto an 18-ml DEAE-Trisacryl M column (BioSepra, Rockland, MA) using a Pharmacia AKTA/fast protein liquid chromatography system. The column was washed with 8 mM Tris acetate, 5 mM magnesium acetate, and 0.1 mM EDTA (pH 7.5), and PDEs eluted with a gradient of 0–1 M sodium acetate in Tris acetate buffer at a flow rate of 1 ml/min into 1.5-ml fractions. [^{3}H]cGMP substrate (0.25 μM; 300,000 dpm) were used to differentiate isozymes, as described previously (23). IC_{50}s were determined using Graphpad Prism software. Reagents were from Sigma (St. Louis, MO), except calmodulin (bovine brain) was from Biomol (Plymouth Meeting, PA).

Orthotopic Rat Tumor Model. Animals were implanted with tumor cells and treated as described earlier (22). Briefly, 6–8-week old female athymic nude rats were obtained from the National Cancer Institute and maintained in pathogen-limited conditions at the Animal Resources Center, University of Colorado Health Sciences Center. One day before the tumor implantation rats were treated with 400 cGy of total body irradiation (Co^{60}) to increase the immunosuppression and the rate of tumor cell implantation. Human A549 adenocarcinoma cells (1 × 10^7 cells in 100 μl of saline) were carefully instilled into the left lung by intratracheal administration through a 3-inch 22-gauge catheter (Popper & Sons, Inc., New Hyde Park, NY) bypassing the trachea and left bronchus of each animal. Rats were anesthetized with Metafane inhalation and held upright at 60° on a slant platform with a rubber band through its incisor teeth. The animals usually recovered from the 2–3 min procedure in <5 min.

Seven days after tumor implantation, rats were randomly divided into groups of 8–15 animals and treated with vehicle solutions (controls) or experimental agents (exisulind and/or docetaxel). Rats were treated with exisulind (25 or 50 mg/kg) by single oral daily gavage with a feeding needle (18-gauge) until the day of sacrifice, alone or in combination with docetaxel. Docetaxel alone or in combination (2.5 or 5 mg/kg) was injected i.p. once per week for 5–6 weeks. One combination group was treated with exisulind (50 mg/kg) and docetaxel 5 mg/kg for three injections followed by three 2.5 mg/kg injections. Body weights of animals were measured once a week, and the animals were monitored closely for clinical signs on a daily basis. On day 21 after tumor implantation, three rats from each group were sacrificed, their lungs were removed, fixed in 10% buffered formalin, and paraffin-embedded. The left lung lobe was longitudinally cut into 5-μm sections, mounted on microscope slides, and stored at room temperature until use.

IHC and TUNEL Analysis. Rat lung tissue slides were processed for either IHC or TUNEL analysis. IHC specimens were dewaxed in xylene and rehydrated through an ethanol series. Endogenous peroxidase activity was eliminated by preincubation in 0.3% H_2O_2. Primary antibodies used following the manufacturers recommended dilution and protocol included: Ki 67 (DAKO, Carpinteria, CA), M30 (Roche), active caspase 3 (Promega), and PDE1 (Fabgennix, Shreveport, LA). Antibodies to PDE5 (peptide sequence AQLYETSLLEN-KRNQV amino acid residues 317–332 in PDE5A1) were raised in sheep, affinity-purified, and used at a dilution of 1:500. The slides were then incubated with an appropriate biotinylated secondary antibody, washed, and incubated with streptavidin-conjugated horseradish peroxidase. The slides were developed using ABC elite 3,3′-diaminobenzidine (Vector), counterstained with hematoxylin, dehydrated through an ethanol and xylene series, and mounted in Permount (Fisher Scientific, Fair Lawn, NJ). TUNEL analysis was performed using the terminal deoxynucleotidyl transferase-FragEL kit (Oncogene Research Products, La Jolla, CA) as per the manufacturer protocol. All of the IHC and TUNEL slides were scored using an Olympus BX-40 microscope. The numbers of positive cells per either 20× (TUNEL, M30 or active caspase 3) or 40× (Ki-67) field of views were scored. Statistics were determined using Graphpad Prism software (one-way ANOVA and Tukey's multiple comparison test).

Results

Exisulind Induces Apoptosis in A549 Cells. The induction and progression of apoptosis can be cell type and condition dependent. Therefore, we investigated exisulind-induced apoptosis in cultured A549 cells using multiple apoptotic markers. Control and exisulind-treated cells were labeled with antibodies to the active form of caspase 3, caspase-cleaved cytokeratin 18, or the p85 fragment of PARP. This allowed us to determine apoptotic levels within treated A549 cells at multiple, early time points along the apoptotic pathway. Previous rat studies have determined that oral administration of exisulind results in serum drug concentrations ranging from 247 to 392 μM (5). Therefore, we treated A549 cells for 5 days with concentrations of exisulind that were under or within that range (100, 200, and 300 μM). To ensure that a representative distribution of the entire cell population was analyzed, both floating and adherent populations were collected and combined before processing. Apoptotic cells were found using all three of the markers (Fig. 1). Apoptotic rates within A549 cells were determined by scoring the number of cells that contained the apoptotic marker per 500 consecutive cells. The data from all three of the apoptotic markers were then averaged together. The A549 apoptosis rates increase in a dose-dependent fashion on treatment with either 100, 200, or 300 μM exisulind. Upon exisulind treatment the average levels of apoptosis increased from a background of 1.3% in the control cells to 2.9, 5.5, and 10.2% in the 100, 200, and 300 μM exisulind treated cultures, respectively (Fig. 1*A*). The increase in apoptosis observed in the 200 and 300 μM exisulind-treated cultures were both significant with *P*s of <0.05 and <0.001, respectively. Representative images using all three of the apoptotic markers are shown in Fig. 1 (*B–E*). These data indicate that exisulind-induced apoptosis in A549 cells occurs at concentrations obtainable within *in vivo* rat serum and can be identified using multiple apoptotic markers.

cGMP PDE Immunoreactivity within Orthotopic A549 Tumors. The relative level of the cGMP PDEs 1 and 5, targets of exisulind, within the orthotopic A549 tumors was determined by IHC analysis. Lung tissue sections from the control group of nude rats containing orthotopic A549 tumors were harvested 21 days after implantation and processed for IHC. Affinity purified polyclonal antibodies specific for PDE1 (all subfamilies) or PDE5 A1 and A2 were used to label the specimens. Tumor cells displayed higher levels of PDE5 immunoreactivity compared with the surrounding normal bronchial epithelial or alveolar cells (Fig. 2*A*). The specificity of the immunoreactivity observed using our PDE5 antibodies was confirmed by comparing labeling intensities of serial lung tumor sections using the affinity-purified serum (Fig. 2*B*) or the serum preincubated with a PDE5 GST fusion protein corresponding to the bovine PDE5 (1) sequence Val^{155}-Asp^{393} (Fig. 2*C*). The vast majority of the labeling is lost after blocking indicating that the observed signal is because of increased levels of PDE5.

The immunolabeling of PDE1 within the lung tumors is also increased compared with normal alveolar cells, albeit not as intensely as PDE5 (Fig. 2*D*). This is not surprising given the high levels of endogenous PDE1 within normal lung tissue (24, 25). These data confirm that there is an increase in the levels of cGMP PDEs within the orthotopic A549 tumors.

PDE Isozyme Expression in A549 Cells and Sensitivity to Exisulind. We identified which PDE isoforms are expressed in the A549 cell line used for the formation of the orthotopic lung tumors. Cell lysates were fractionated by anion-exchange chromatography (Fig. 3*A*) and found to express three peaks of cGMP PDE activity. The first peak of activity (fraction 30) was activated by calcium and calmodulin, indicative of PDE1 isoform activity (Fig. 3*B*). The second peak (fraction 48) contained overlap from the first and third peaks, but also was partially inhibited with 100 nM of the PDE5-specific inhibitor E4021. The location of this second peak matched that seen previously for PDE5 from SW480 and HT29 colon cell lines, and the HT1376 bladder cell lines (3, 7, 13). Much of the cAMP PDE activity was inhibited by 10 μM rolipram, a PDE4-specific inhibitor. The cAMP activity

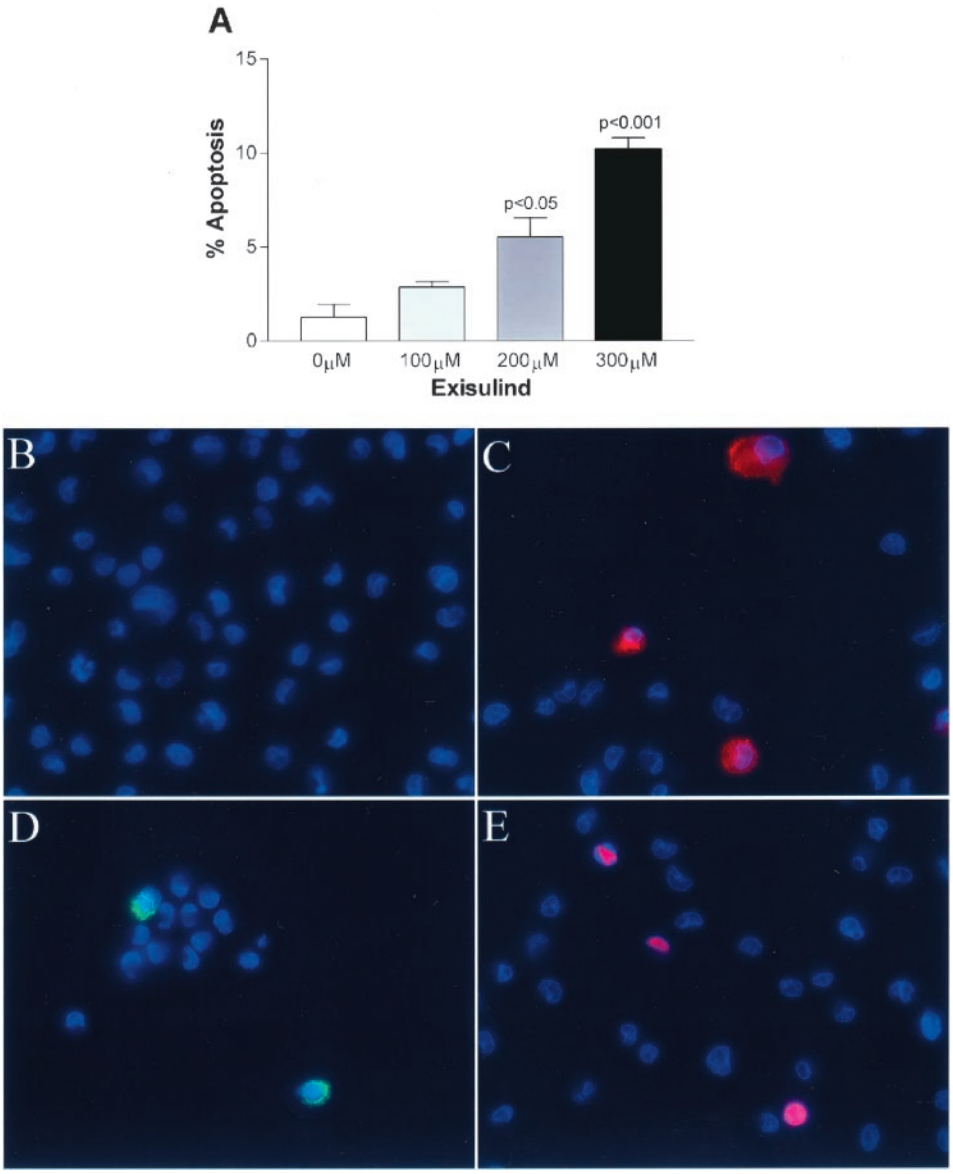

Fig. 1. Exisulind-induced apoptosis in A549 cell cultures. A549 cells were treated with 100, 200, or 300 μM exisulind for 5 days (*A*). Apoptosis was quantified by scoring the number of positive cells per 500 consecutive cells that labeled with either of the three apoptotic markers: active caspase 3 (AC3), caspase cleaved cytokeratin 18 (M30), and p85 PARP fragment. The percentage of apoptosis for each dose of exisulind was obtained by averaging the data from the three apoptotic markers. Statistical significance is relative to control (0% exisulind) cultures. Representative images of apoptotic A549 cells identified by each marker are shown (*B–E*). Cells were treated with either 0.1% DMSO (*B*) or 600 μM exisulind for 24 h (*C–E*). Apoptotic cells were identified using antibodies to active caspase 3 (*B* and *C*), caspase cleaved cytokeratin 18 (*D*), and p85 PARP fragment (*E*). All of the cells were counterstained with 4′,6-diamidino-2-phenylindole; *bars,* ±SD.

that was not inhibited by rolipram coincided with the third peak of cGMP PDE activity (fraction 72). Addition of 5 μM cGMP showed inhibition of the cAMP activity consistent with the presence of the dual substrate isoform PDE3. In addition, the PDE3 selective inhibitors of 1 μM cilostamide and 1 nM trequinsin inhibited ~60% of the cGMP PDE activity (data not shown). High concentrations of exisulind (600 μM) inhibited most of the cGMP PDE activity from each of the three peaks even in the presence of calcium/calmodulin. PDE1 from fractions 24–33 when tested for exisulind inhibition on calcium/calmodulin activated cGMP PDE showed an IC_{50} of 70 μM (inset). Exisulind tested on the second peak with some overlap from the other peaks showed an IC_{50} of 110 μM (data not shown) similar to that seen previously for PDE5 from SW480, HT29, and HT1376 (3, 7, 13).

Drug-induced Apoptosis in Orthotopic A549 Tumors. The apoptotic indexes in the orthotopic tumors from all of the treatment groups were determined in a manner similar to that performed on the A549 cells *in vitro*. Three independent apoptotic markers identified apoptotic cells: antibody markers to active caspase 3 and caspase cleaved cytokeratin 18, and enzymatic TUNEL analysis to identify apoptotic cells containing fragmented DNA. Three rats from each treatment group were sacrificed 21 days after initiation of exisulind and/or docetaxel treatment. Tissue sections from all of the treatment groups were processed for each apoptotic marker and the number of positive apoptotic cells per ×20 field of view scored. Data were collected from 6 to 8 independent fields of view for each tumor sample. Fig. 4 contains representative images obtained using an antibody to caspase-cleaved cytokeratin 18, from the control, high-dose exisulind,

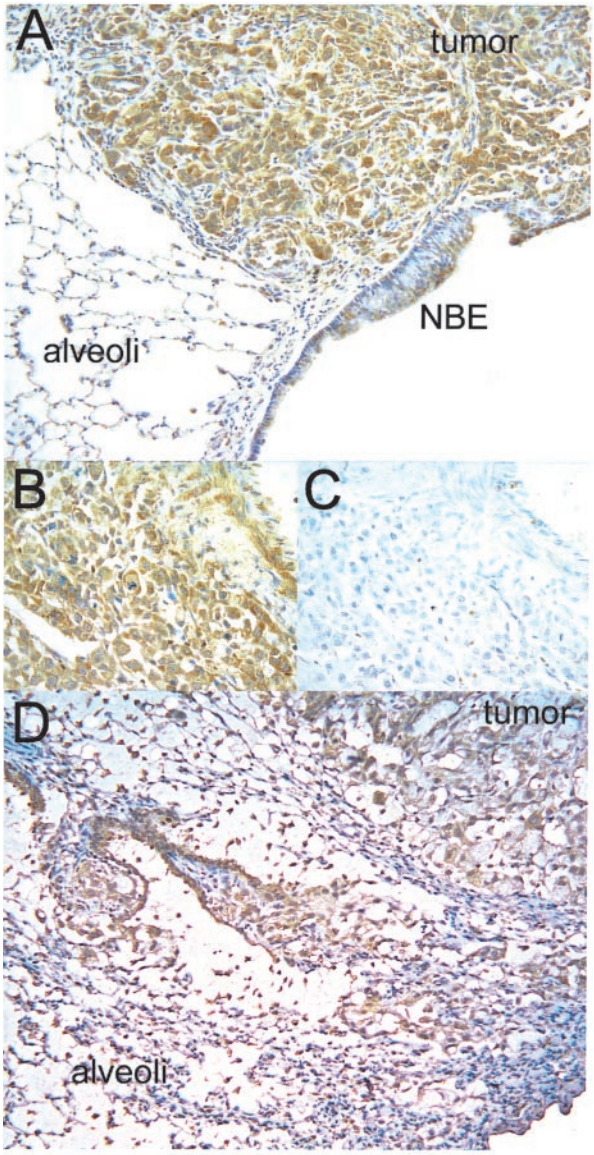

Fig. 2. PDE5 and 1 expression within orthotopic A549 tumor cells. Rat lung tissue sections containing orthotopic A549 tumors were processed for IHC and labeled with a PDE5 or PDE1 antibody as described in "Materials and Methods." *A,* A549 tumor cells displayed higher levels of PDE 5 immunoreactivity compared with normal surrounding bronchial epithelium and alveolar cells. The specificity of the PDE5 antibody was confirmed by comparing the labeling of serial sections with the affinity purified serum without (*B*) or with (*C*) preincubation with an antigen containing PDE5-GST fusion protein. The vast majority of the tumor labeling was eliminated on preincubation of the PDE5 antibody with the PDE5-GST fusion protein. PDE1 immunoreactivity was also increased in orthotopic A549 tumors compared with surrounding normal lung tissue (*D*).

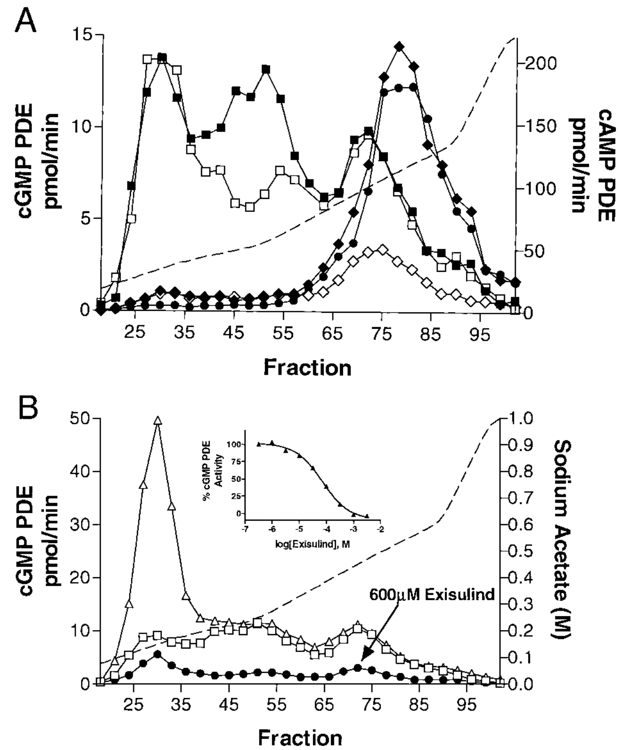

Fig. 3. Cyclic nucleotide PDE isozymes in A549 cells and inhibition by exisulind. High-speed supernatants from homogenized A549 cells were chromatographed on a DEAE-Trisacryl M column and eluted with a gradient of 0–1 M sodium acetate buffer at 1 ml/min into 1.5 ml fractions as described in "Materials and Methods." PDE activity was determined with 0.25 μM [^{3}H]cGMP substrate or 0.25 μM [^{3}H]cAMP substrate. *A,* cGMP PDE activity (■) 100 nM E4021 (□). cAMP PDE activity (♦) was measured 10 μM rolipram (◇) or with 5 μM cGMP (●). *B,* All assays were run in the presence of 0.5 mM EGTA to bind calcium. Without calcium/calmodulin, this showed the unactivated cGMP PDE1 activity (□). Addition of 2 mM calcium and 150 nM calmodulin activated the PDE1 (△). In the presence of calcium and calmodulin, 600 μM exisulind inhibited the three peaks of cGMP PDE activity (●). The PDE1 fractions 24–33 were pooled, and exisulind inhibition was tested on calcium calmodulin-activated PDE1 and gave an IC_{50} of 70 μM (*inset*).

high-dose docetaxel, and the high-dose exisulind/docetaxel combination. Tissues labeled with antiactive caspase 3 antibodies or TUNEL gave similar images (data not shown). All three of the markers indicate that there was an increase in apoptosis, compared with controls, on treatment with exisulind and docetaxel. The apoptotic levels determined from each of the three markers for each treatment group is shown in Fig. 5, *A–C*. Treatment with exisulind and/or docetaxel resulted in a dose-dependent increase in the number of apoptotic cells as determined by each apoptotic marker. To quantify the cumulative apoptosis levels in all of the treatment groups using all three of the apoptosis markers, the data obtained from each individual marker was normalized relative to its own untreated control group and averaged between all three of the apoptosis markers. The resultant cumulative apoptotic index showed an exisulind dose-dependent increase in apoptosis (Fig. 5*D*). In addition, each treatment group showed increased apoptosis in the lung tumors when comparing higher *versus* lower exisulind doses. As single agents, exisulind-induced apoptosis was consistently higher than that observed for docetaxel. Additionally, exisulind increased the apoptotic rates at both doses with or without docetaxel treatment.

Only non-necrotic areas of the tumors were analyzed to ensure that only true apoptotic cells were scored. The percentage of each tumor that was necrotic within the control, high-dose exisulind, high-dose docetaxel, and the high-dose

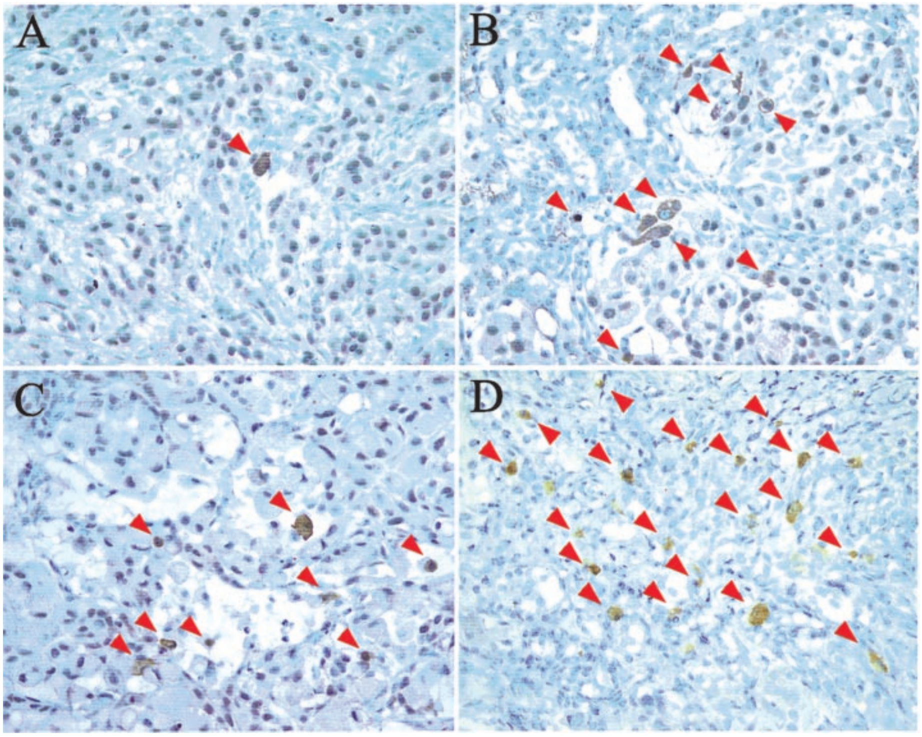

Fig. 4. Exisulind increases *in vivo* apoptosis levels. Rat lung tissue sections containing orthotopic A549 tumors from each treatment group were prepared as described in "Materials and Methods" and labeled with three independent apoptotic markers. Representative images using an antibody specific for caspase-cleaved cytokeratin 18 are shown for the control (*A*), high-dose exisulind 50 mg/kg (*B*), high-dose docetaxel 5 mg/kg (*C*), and the combined high-dose exisulind and docetaxel (*D*).

exisulind/docetaxel combination groups were measured. Across the treatment groups necrosis ranged from 7.8 to 18.5% and was not statistically significant.

Docetaxel but not Exisulind Decreases the Proliferation Rate within Orthotopic A549 Tumors. The effects of exisulind and docetaxel on *in vivo* proliferation within the orthotopic A549 lung tumors were investigated by labeling tumor sections from all of the treatment groups with the proliferation marker Ki-67. Animals treated with 2.5 or 5.0 mg/kg docetaxel had a significant decrease in the number of proliferating cells. These observations were quantified by scoring the number of Ki-67-positive cells per ×40 field of view. The docetaxel effect was 21.5% inhibition with the lower dose (2.5 mg/kg) and 48.5% at the higher dose (5.0 mg/kg). Exisulind at either 25 or 50 mg/kg/day resulted in no significant decrease in the number of Ki-67-positive cells. Representative images from the control, exisulind 50 mg/kg, docetaxel 5 mg/kg, and combination exisulind 50 mg/kg docetaxel 5 mg/kg are shown in Fig. 6, *A–D*. Animals treated with a combination of both exisulind and docetaxel did not show an additional decrease in proliferation over that observed with the corresponding docetaxel treatment alone. Therefore, in this *in vivo* orthotopic model, exisulind does not lower the proliferative rate of the A549 tumor cells. The proliferation data for all of the treatment groups are summarized in Fig. 6*E*.

Discussion

These studies report that exisulind treatment of human NSCLC A549 cells grown in culture or administration to *in vivo* orthotopic tumors in a nude rat model increased apoptotic indexes. Determination of apoptosis was designed to minimize artifacts specific to a single apoptotic marker. The current standard of identifying apoptotic cells involves demonstration of specific oligonucleosomal DNA fragments either by double antibody ELISA or enzymatic TUNEL analysis. However, this method can give inaccurate results because of necrotic cells with fragmented DNA, early apoptotic cells lacking digested DNA, variation in sample preparation, and enzymatic activity (26–28). Recent reports also indicate potential shortcomings of relying on only the TUNEL apoptotic marker when quantifying apoptosis within tissue sections (29–31). To obviate these problems antibodies to specific apoptotic proteins present at various stages of the apoptotic pathway were used. Specifically, the active form of caspase 3 and caspase-cleaved cytokeratin 18 were studied. As expected, the specific number of apoptotic cells identified by each individual marker varied one to another; however, each marker indicated that the indexes for both *in vitro* and *in vivo* apoptosis increased in a dose-dependent fashion after exisulind exposure. These studies establish that apoptosis is induced by exisulind administration in A549 cells of *in vivo* tumors, as has been seen in numerous cancer cell lines.

Apoptosis, once initiated, is a relatively rapid event, and any resultant apoptotic bodies are engulfed by phagocytosis in a short period of time (32, 33). Therefore, within the orthotopic A549 tumors it is relatively difficult to identify the rare cells actively undergoing apoptosis. This would imply that the exisulind-induced increases in the *in vivo* apoptosis levels might be conservative indexes of its effects. Consequently, even moderate increases in apoptosis observed in a

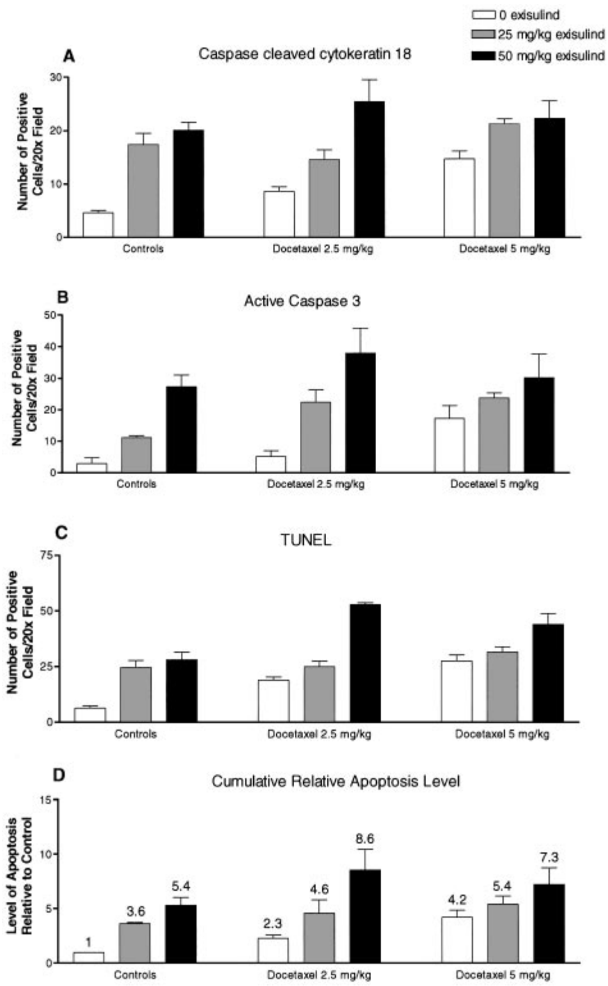

Fig. 5. *In vivo* apoptosis quantification. Lung tissue sections from all treatment groups prepared as described in "Materials and Methods" were labeled using antibodies to either active caspase 3 or caspase-cleaved cytokeratin 18. Apoptotic cells were also identified by TUNEL analysis. The number of apoptotic cells per ×20 fields of view were scored for each lung tumor. An average of seven fields of view were scored in each tumor. The number of apoptotic cells positive for each marker are shown (*A–C*). With each marker, the number of apoptotic cells increases in a dose-dependent fashion with exisulind treatment. The combined fold apoptosis levels were determined by normalizing the fold increase in apoptosis of each individual marker as compared with their own control levels. The resulting fold apoptosis increase for each marker were averaged together to give relative cumulative apoptosis index for each drug treatment group (*D*); *bars,* ±SD.

single tissue section may only be a fraction of the total apoptotic effect occurring within the tumor as a whole. The variables inherent in this type of *in vivo* apoptotic analysis dictate that the results be interpreted with a degree of caution. The fact that the apoptotic rates of combination treated groups were not exactly additive of the single treatment groups illustrates this point. A reduced quantitative correlation may be attributable simply to the inherent variability of data collection within an *in vivo* system. However, additional mechanisms beside apoptosis induction or proliferation inhibition active within this model may be indicated. For example, in future studies it would be informative to determine whether the exisulind/docetaxel combination exhibits any antiangiogenic activity.

We note that the *in vivo* apoptosis data were generated from tissues harvested at a single (day 21) time point. This collection date was selected with the rationale of harvesting tissues before any deaths occurred in the control group but allowing enough treatment time to show a molecular drug effect within the tumors. Additional analyses are required to determine when the drug initiates apoptosis in the tumors. It is possible that the high-dose combination groups increased their apoptosis levels quicker than the low-dose groups and, therefore, by day 21 the window of maximal apoptosis in the high-dose treatment groups may have passed. The lack of a statistical difference between the levels of apoptosis in the 5 mg/kg docetaxel plus 25 mg/kg or 50 mg/kg exisulind may reflect variable time courses.

The concentrations of exisulind used in our *in vitro* cell culture apoptosis analysis correlates with serum levels obtained in a previous rat cancer model (5). In the rat colon cancer model, exisulind serum levels of 346 μM were obtained without any observable weight decreasing toxicity. Our ability to induce apoptosis in A549 cells beginning with concentrations of 100 μM exisulind also correlates with the IC_{50} for PDE1 and 5 inhibition of 70 μM and 110 μM, respectively. The correlation between the increases in apoptosis within cultured A549 cells *in vitro* and the increases in apoptosis seen within the A549 orthotopic tumors *in vivo* is of importance, because it provides support for extrapolating the observations seen in culture to potential biological effects predicting *in vivo* drug activity. These data suggest that the inhibition of PDE1 and 5 by exisulind can induce apoptosis in both an *in vitro* and *in vivo* environment. In A549 cells exisulind also inhibits PDE1 expressed in this lung tumor along with PDE5 to prevent cGMP hydrolysis in this NSCLC model. This is supported by previous reports of exisulind inhibiting the cGMP hydrolysis by PDE family members including PDE2 and 5 in colon, pancreatic, and bladder cancer cell lines. In colon cancer cells the inhibition of cGMP PDE activity on exisulind treatment results in a sustained increase in cGMP, but not cAMP levels within the cells (7). This sustained cGMP elevation activates PKG, which plays a critical role in the mechanism by which exisulind induces apoptosis. To date, two direct effects of exisulind-dependent PKG activation have been described: first, the attenuation of β-catenin levels within cells treated with exisulind (7, 15). This facilitates a decrease in both nuclear and cytoplasmic levels of β-catenin through degradation by ubiquitin-dependent proteolysis. Second, PKG directly phosphorylates mitogen-activated protein kinase kinase kinase 1, which leads to the downstream activation of c-Jun NH_2-terminal kinase 1 (13, 14, 34). Both of these molecular effects of exisulind lead to the induction of apoptosis. Our data show that A549 cells contain elevated levels of cGMP PDEs 1 and 5, and that exisulind inhibits their hydrolytic activity. Therefore, the subsequent induction of apoptosis in A549 cells is likely because of a mechanism of action similar to that observed in colon cancer cells.

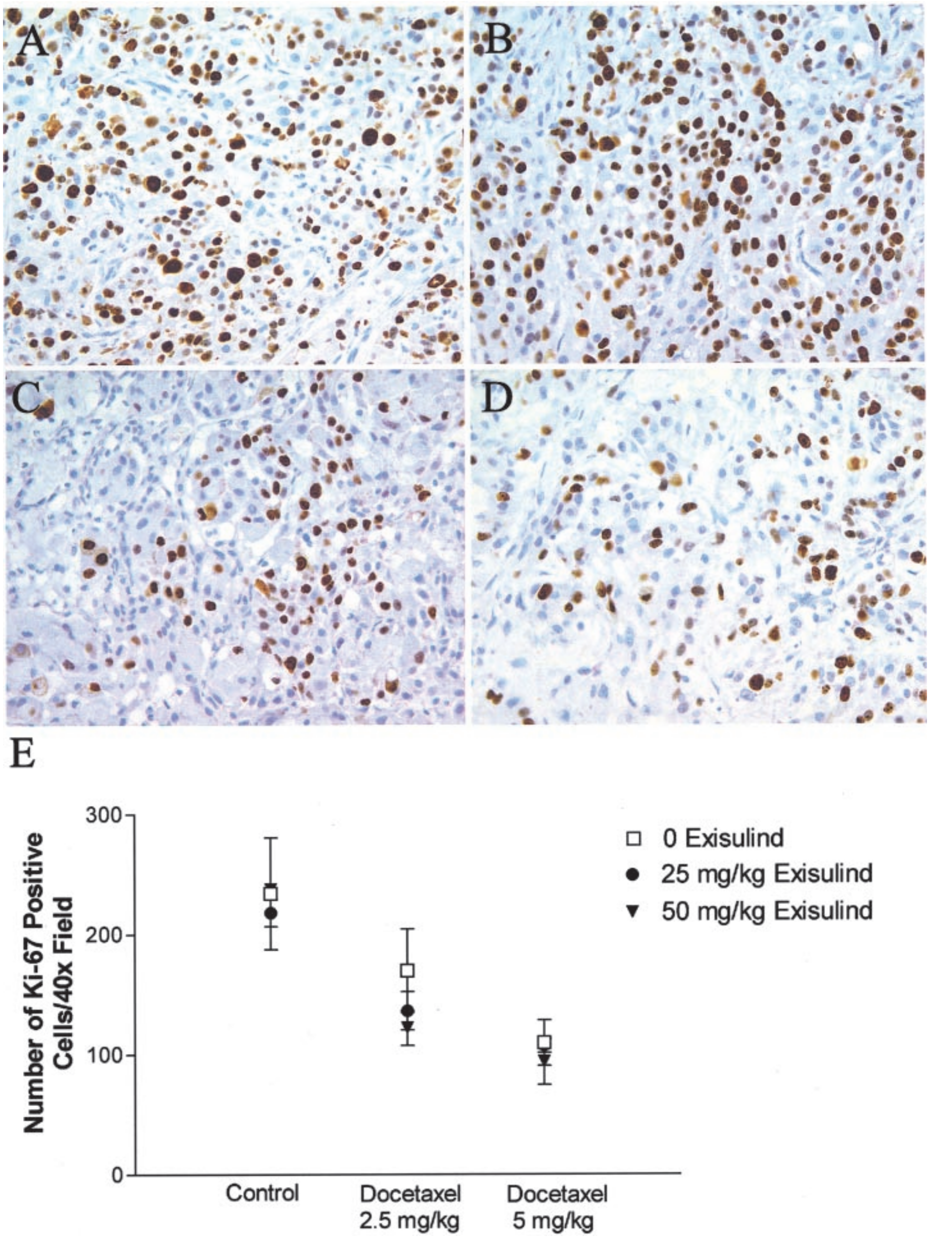

Fig. 6. Docetaxel but not exisulind decrease *in vivo* proliferation. Rat lung tissue sections containing orthotopic A549 tumors from all treatment groups prepared as in "Materials and Methods" were labeled with an antibody to Ki-67, a marker of proliferation. Representative images are shown from the control (*A*), high-dose exisulind 50 mg/kg (*B*), high-dose docetaxel 5 mg/kg (*C*), and the combination high-dose exisulind and docetaxel groups (*D*). The number of Ki-67-positive cells decreases on docetaxel but not exisulind treatment. This effect was quantified by scoring the number of Ki-67-positive cells per ×40 field of view. Ten fields of view were scored in each tumor. The data for all treatment groups are presented (*E*); *bars,* ±SD.

Docetaxel exhibits two major biological effects: the first being decreased proliferation because of direct binding to and stabilization of microtubules causing a G_2/M block (35) and the second being apoptosis induction. The data obtained using the proliferation marker Ki-67 indicate that exisulind and docetaxel have disparate effects on *in vivo* tumor proliferation rates. Neither dose of exisulind used in this study lowered the proliferative rate within the tumors. In contrast, docetaxel lowered the proliferative rate within the tumor. Rats treated with the combination of exisulind and docetaxel displayed proliferative rates similar to rats treated with docetaxel alone. Therefore, exisulind does not affect the gross proliferative rate of A549 orthotopic tumors *in vivo*.

We reported previously an increase in survival of nude rats harboring orthotopic A549 tumors that were treated with a combination of exisulind (50 mg/kg/day) and docetaxel (5 mg/kg). In the same study rats treated with either exisulind at 25 or 50 mg/kg/day, or those treated with docetaxel at 2.5 or 5 mg/kg alone or in low-dose combinations did not survive significantly longer than control rats. As single agents the biological effects of docetaxel (decrease in proliferation) or exisulind (increase in apoptosis) were not sufficient to increase survival. However, these studies show that the treatment group with the highest survival (exisulind 50 mg/kg and docetaxel 5 mg/kg) had an exisulind-dependent increased apoptosis rate coupled with a docetaxel-dependent decreased proliferative rate. As commonly observed in the clinical setting, the growth rate of the A549 tumors and metastasis in this model could only be overcome through the combined effects of these compounds. These data support the use of combining exisulind and docetaxel as a rationale combination to increase apoptosis and decrease proliferation as a treatment for NSCLC.

References

1. Thompson, H. J., Jiang, C., Lu, J., Mehta, R. G., Piazza, G. A., Paranka, N. S., Pamukcu, R., and Ahnen, D. J. Sulfone metabolite of sulindac inhibits mammary carcinogenesis. Cancer Res., *57:* 267–271, 1997.

2. Piazza, G. A., Rahm, A. K., Finn, T. S., Fryer, B. H., Li, H., Stoumen, A. L., Pamukcu, R., and Ahnen, D. J. Apoptosis primarily accounts for the growth-inhibitory properties of sulindac metabolites and involves a mechanism that is independent of cyclooxygenase inhibition, cell cycle arrest, and p53 induction. Cancer Res., *57:* 2452–2459, 1997.

3. Piazza, G. A., Thompson, W. J., Pamukcu, R., Alila, H. W., Whitehead, C. M., Liu, L., Fetter, J. R., Gresh, W. E., Jr., Klein-Szanto, A. J., Farnell, D. R., Eto, I., and Grubbs, C. J. Exisulind, a novel proapoptotic drug, inhibits rat urinary bladder tumorigenesis. Cancer Res., *61:* 3961–3968, 2001.

4. Lim, J. T., Piazza, G. A., Han, E. K., Delohery, T. M., Li, H., Finn, T. S., Buttyan, R., Yamamoto, H., Sperl, G. J., Brendel, K., Gross, P. H., Pamukcu, R., and Weinstein, I. B. Sulindac derivatives inhibit growth and induce apoptosis in human prostate cancer cell lines. Biochem. Pharmacol., *58:* 1097–1107, 1999.

5. Piazza, G. A., Alberts, D. S., Hixson, L. J., Paranka, N. S., Li, H., Finn, T., Bogert, C., Guillen, J. M., Brendel, K., Gross, P. H., Sperl, G., Ritchie, J., Burt, R. W., Ellsworth, L., Ahnen, D. J., and Pamukcu, R. Sulindac sulfone inhibits azoxymethane-induced colon carcinogenesis in rats without reducing prostaglandin levels. Cancer Res., *57:* 2909–2915, 1997.

6. Goluboff, E. T., Shabsigh, A., Saidi, J. A., Weinstein, I. B., Mitra, N., Heitjan, D., Piazza, G. A., Pamukcu, R., Buttyan, R., and Olsson, C. A. Exisulind (sulindac sulfone) suppresses growth of human prostate cancer in a nude mouse xenograft model by increasing apoptosis. Urology, *53:* 440–445, 1999.

7. Thompson, W. J., Piazza, G. A., Li, H., Liu, L., Fetter, J., Zhu, B., Sperl, G., Ahnen, D., and Pamukcu, R. Exisulind induction of apoptosis involves guanosine 3′,5′-cyclic monophosphate phosphodiesterase inhibition, protein kinase G activation, and attenuated β-catenin. Cancer Res., *60:* 3338–3342, 2000.

8. Piazza, G. A., Klein-Szanto, A. J., Ahnen, D. J., Li, H., Liu, L., David, M., Pamukcu, R., and Thompson, W. J. Overexpression of cGMP phosphodiesterase (cG PDE) in colonic neoplasias compared to normal mucosa. Gastroenterology, *118* (Suppl. 2)*:* A282, 2000.

9. Piazza, G. A., Klein-Szanto, A. J., Xu, A., Pamukcu, R., and Thompson, W. J. Phosphodiesterase 5 overexpression in human non-small cell lung tumors compared to normal bronchial epithelium. Proc. Am. Assoc. Cancer Res., *42:* 811, 2001.

10. Piazza, G. A., Sperl, G., Whitehead, C. M., Xu, S., Klein-Szanto, A. J., Yip-Sneider, M. T., Sweeney, C. J., Lloyd, M., Liu, L., Fetter, J., Pamukcu, R., and Thompson, W. J. Cyclic GMP phosphodiesterase (cG PDE) overexpression in human pancreatic carcinomas and a target for selective apoptotic antineoplastic drugs. Gastroenterology, *120* (Suppl. 1)*:* A75, 2001.

11. Liu, L., Underwood, T., Li, H., Pamukcu, R., and Thompson, W. J. Specific cGMP binding by the cGMP binding domains of cGMP-binding cGMP specific phosphodiesterase. Cell. Signal., *14:* 45–51, 2002.

12. Liu, L., Li, H., Underwood, T., Lloyd, M., David, M., Sperl, G., Pamukcu, R., and Thompson, W. J. Cyclic GMP-dependent protein kinase activation and induction by exisulind and CP461 in colon tumor cells. J. Pharmacol. Exp. Ther., *299:* 583–592, 2001.

13. Soh, J. W., Mao, Y., Kim, M. G., Pamukcu, R., Li, H., Piazza, G. A., Thompson, W. J., and Weinstein, I. B. Cyclic GMP mediates apoptosis induced by sulindac derivatives via activation of c-Jun NH2-terminal kinase 1. Clin. Cancer Res., *6:* 4136–4141, 2000.

14. Soh, J. W., Mao, Y., Liu, L., Thompson, W. J., Pamukcu, R., and Weinstein, I. B. Protein kinase G activates the JNK1 pathway via phosphorylation of MEKK1. J. Biol. Chem., *276:* 16406–16410, 2001.

15. Li, H., Liu, L., David, M., Whitehead, C. M., Chen, M., Fetter, J., Sperl, G., Pamukcu, R., and Thompson, W. J. Pro-apoptotic actions of exisulind and CP461 in SW480 colon tumor cells involve β-catenin and cyclin D1 down regulation. Biochem. Pharmacol., *64:* 1325–1336, 2002.

16. Greenlee, R. T., Hill-Harmon, M. B., Murray, T., and Thun, M. Cancer statistics, 2001. CA Cancer J. Clin., *51:* 15–36, 2001.

17. Fossella, F. V., DeVore, R., Kerr, R. N., Crawford, J., Natale, R. R., Dunphy, F., Kalman, L., Miller, V., Lee, J. S., Moore, M., Gandara, D., Karp, D., Vokes, E., Kris, M., Kim, Y., Gamza, F., and Hammershaimb, L. Randomized phase III trial of docetaxel versus vinorelbine or ifosfamide in patients with advanced non-small-cell lung cancer previously treated with platinum-containing chemotherapy regimens. The TAX 320 Non-Small Cell Lung Cancer Study Group. J Clin. Oncol., *18:* 2354–2362, 2000.

18. Roszkowski, K., Pluzanska, A., Krzakowski, M., Smith, A. P., Saigi, E., Aasebo, U., Parisi, A., Pham, T. N., Olivares, R., and Berille, J. A multicenter, randomized, phase III study of docetaxel plus best supportive care versus best supportive care in chemotherapy-naive patients with metastatic or non-resectable localized non-small cell lung cancer (NSCLC). Lung Cancer, *27:* 145–157, 2000.

19. Shepherd, F. A., Dancey, J., Ramlau, R., Mattson, K., Gralla, R., O'Rourke, M., Levitan, N., Gressot, L., Vincent, M., Burkes, R., Coughlin, S., Kim, Y., and Berille, J. Prospective randomized trial of docetaxel versus best supportive care in patients with non-small-cell lung cancer previously treated with platinum-based chemotherapy. J. Clin. Oncol., *18:* 2095–2103, 2000.

20. Bunn, P. A., Jr., and Kelly, K. New chemotherapeutic agents prolong survival and improve quality of life in non-small cell lung cancer: a review of the literature and future directions. Clin. Cancer Res., *4:* 1087–1100, 1998.

21. Soriano, A. F., Helfrich, B., Chan, D. C., Heasley, L. E., Bunn, P. A., Jr., and Chou. T. C. Synergistic effects of new chemopreventive agents and conventional cytotoxic agents against human lung cancer cell lines. Cancer Res., *59:* 6178–6184, 1999.

22. Chan, D. C., Earle, K. A., Zhao, T. L., Helfrich, B., Zeng, C., Baron, A., Whitehead, C. M., Piazza, G., Pamukcu, R., Thompson, W. J., Alila, H., Nelson, P., and Bunn, P. A., Jr. Exisulind in combination with docetaxel inhibits growth and metastasis of human lung cancer and prolongs survival in athymic nude rats with orthotopic lung tumors. Clin. Cancer Res., *8:* 904–912, 2002.

23. Thompson, W. J., Terasaki, W. L., Epstein, P. M., and Strada, S. J. Assay of cyclic nucleotide phosphodiesterase and resolution of multiple molecular forms of the enzyme. Adv. Cyclic Nucleotide Res., *10:* 69–92, 1979.

24. Sharma, R. K., and Wang, J. H. Purification and characterization of bovine lung calmodulin-dependent cyclic nucleotide phosphodiesterase. An enzyme containing calmodulin as a subunit. J. Biol. Chem., *261:* 14160–14166, 1986.

25. Sharma, R. K., and Kalra, J. Characterization of calmodulin-dependent cyclic nucleotide phosphodiesterase isoenzymes. Biochem. J, *299* (Pt 1)*:* 97–100, 1994.

26. Hall, P. A. Assessing apoptosis: a critical survey. Endocr. Relat. Cancer, *6:* 3–8, 1999.

27. Darzynkiewicz, Z., Bedner, E., Traganos, F., and Murakami, T. Critical aspects in the analysis of apoptosis and necrosis. Hum. Cell, *11:* 3–12, 1998.

28. Collins, R. J., Harmon, B. V., Gobe, G. C., and Kerr, J. F. Internucleosomal DNA cleavage should not be the sole criterion for identifying apoptosis. Int. J. Radiat. Biol., *61:* 451–453, 1992.

29. Willingham, M. C. Cytochemical methods for the detection of apoptosis. J. Histochem. Cytochem., *47:* 1101–1110, 1999.

30. Walker, J. A., and Quirke, P. Viewing apoptosis through a 'TUNEL'. J. Pathol., *195:* 275–276, 2001.

31. Barrett, K. L., Willingham, J. M., Garvin, A. J., and Willingham, M. C. Advances in cytochemical methods for detection of apoptosis. J. Histochem. Cytochem., *49:* 821–832, 2001.

32. Coles, H. S., Burne, J. F., and Raff, M. C. Large-scale normal cell death in the developing rat kidney and its reduction by epidermal growth factor. Development (Camb.), *118:* 777–784, 1993.

33. Green, D. R., and Beere, H. M. Apoptosis. Mostly dead. Nature (Lond.), *412:* 133–135, 2001.

34. Alberts, D. S., Hixson, L., Ahnen, D., Bogert, C., Einspahr, J., Paranka, N., Brendel, K., Gross, P. H., Pamukcu, R., and Burt, R. W. Do NSAIDs exert their colon cancer chemoprevention activities through the inhibition of mucosal prostaglandin synthetase? J. Cell Biochem., *22* (Suppl.)*:* 18–23, 1995.

35. Vaishampayan, U., Parchment, R. E., Jasti, B. R., and Hussain, M. Taxanes: an overview of the pharmacokinetics and pharmacodynamics. Urology, *54:* 22–29, 1999.

Exisulind-induced Apoptosis in a Non-Small Cell Lung Cancer Orthotopic Lung Tumor Model Augments Docetaxel Treatment and Contributes to Increased Survival

Clark M. Whitehead, Keith A. Earle, John Fetter, et al.

Mol Cancer Ther 2003;2:479-488.